Provided for non-commercial research and education use.
Not for reproduction, distribution or commercial use.

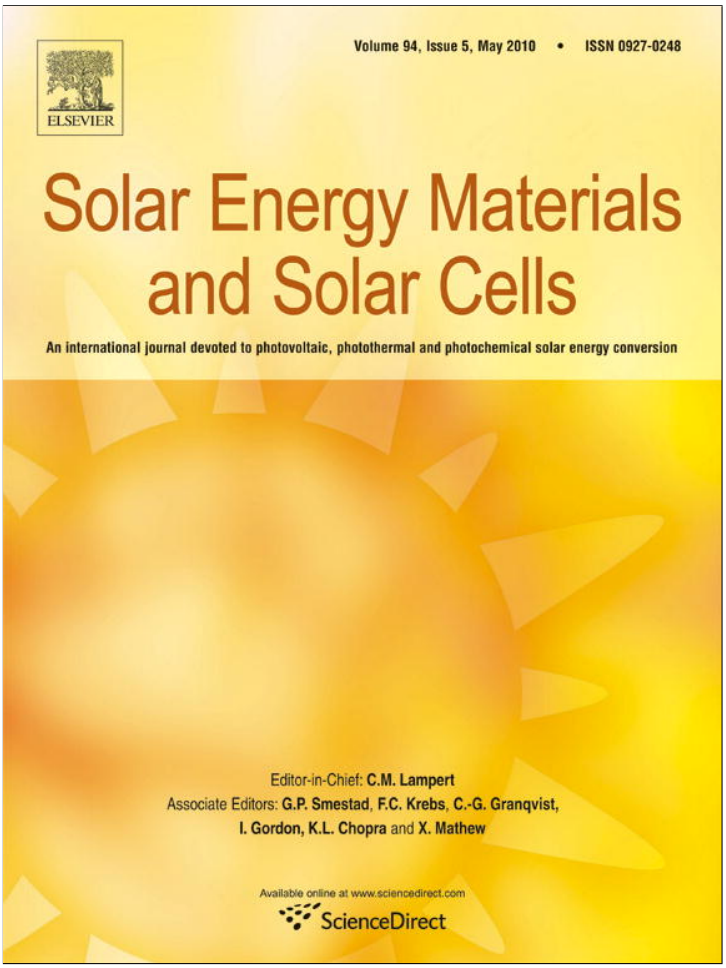

This article appeared in a journal published by Elsevier. The attached copy is furnished to the author for internal non-commercial research and education use, including for instruction at the authors institution and sharing with colleagues.

Other uses, including reproduction and distribution, or selling or licensing copies, or posting to personal, institutional or third party websites are prohibited.

In most cases authors are permitted to post their version of the article (e.g. in Word or Tex form) to their personal website or institutional repository. Authors requiring further information regarding Elsevier's archiving and manuscript policies are encouraged to visit:

http://www.elsevier.com/copyright

Author's personal copy

Solar Energy Materials & Solar Cells 94 (2010) 750–754

Contents lists available at ScienceDirect

Solar Energy Materials & Solar Cells

journal homepage: www.elsevier.com/locate/solmat

Effect of hybrid carbon nanotubes–bimetallic composite particles on the performance of polymer solar cells

Sun-Young Park [a,b], Whi-Dong Kim [c], Do-Geun Kim [a], Jong-Kuk Kim [a], Yong-Soo Jeong [a], Joo Hyun Kim [b], Jae Keun Lee [d], Soo H. Kim [c,*], Jae-Wook Kang [a]

[a] Department of Material Processing, Korea Institute of Materials Science, Changwon 641-831, Republic of Korea
[b] Division of Applied Chemical Engineering, Department of Polymer Engineering, Pukyong National University, Busan 608-739, Republic of Korea
[c] Department of Nanosystem and Nanoprocess Engineering, Pusan National University, 30 Jangjeon-dong, Geumjeong-gu, Busan 609-735, Republic of Korea
[d] School of Mechanical Engineering, Pusan National University, 30 Jangjeon-dong, Geumjeong-gu, Busan 609-735, Republic of Korea

ARTICLE INFO

Article history:
Received 21 August 2009
Received in revised form
17 December 2009
Accepted 19 December 2009
Available online 15 January 2010

Keywords:
Carbon nanotubes
Organic photovoltaic cell
Bimetallic nanoparticles
Current density
Power conversion efficiency

ABSTRACT

Hybrid carbon nanotubes–bimetallic composite nanoparticles with sea urchin-like structures (SU-CNTs) were introduced to bulk heterojuction polymer-fullerene solar cells to improve their performance. The SU-CNTs were composed of multi-walled CNTs, which were grown radially over the entire surface of the bimetallic nanoparticles composed of Ni and Al. SU-CNTs with a precisely controlled length of $\sim 200 \pm 40$ nm were dispersed homogenously in a polymer active layer. Compared with a pristine device (i.e., without SU-CNTs), the SU-CNTs-doped organic photovoltaic (OPV) cells showed an improved short-circuit current density and power conversion efficiency from 7.5 to 9.5 mA/cm^2 and $2.1 \pm 0.1\%$ to $2.2 \pm 0.2\%$ (max. 2.5%), respectively. The specially designed SU-CNTs have strong potential as an effective exciton dissociation medium in the polymer active layer to enhance the performance of organic solar cells.

© 2009 Elsevier B.V. All rights reserved.

1. Introduction

Solar cell is a potential renewable energy system that converts sunlight to electrical power directly. Among the various types of solar cells, the industrial applications of inorganic solar cells (e.g., silicon-based solar cells) to replace non-renewable energy sources are still limited because of their high fabrication cost. Unlike inorganic solar cells, organic photovoltaic (OPV) cells have attracted considerable attention due to the advantages of flexible, light-weight, and low-cost applications of solar energy conversion [1–7]. Tang [1] reported the development of an OPV with a power conversion efficiency (PCE) of ~1% based on a single donor–acceptor heterojunction. Since then, the PCE has been improved steadily to approximately 5% by many research groups [8–11]. In addition, according to the results of a recent computer simulation, the PCE of OPV cells is predicted to reach 10% by optimizing the donor/acceptor energy levels [12].

The PCE of bulk-heterojunction (BHJ) polymer photovoltaic cells is associated with the open-circuit voltage (V_{oc}), short-circuit current (J_{sc}), and fill factor (FF) delivered by these devices under sunlight illumination. Recently, it was demonstrated that the V_{oc} of BHJ devices is related to the highest occupied molecular orbital (HOMO) level of the donor [12]. New polymers with a high oxidation potential are needed to increase the V_{oc}. On the other hand, the current density is related directly to the exciton dissociation rate and charge mobility in semiconducting materials, in which the exciton dissociation between donor and acceptor materials should be maximized and sufficient charge collection should be made at the electrodes.

With an aim of improving the performance of OPVs, carbon nanotubes (CNTs) have been introduced recently to OPV devices [13]. The CNTs are used as electrodes [14–16], layered at a desired location [17] or blended with a polymer [13,18–20] as BHJ devices. This is because CNTs are not only optically transparent, flexible and environmentally resistant, they also have strong potentials as exciton dissociating centers and conducting agents with high carrier mobility [18]. However, the applications and characterization of CNTs in these OPV devices have been limited due to the difficulties in incorporating CNTs in polymers. In general, there are two ways of incorporating CNTs in a BHJ device configuration: (i) layer-by-layer assembly of layer-by-layer of CNTs/polymer at the desired locations or (ii) fabrication of a hybrid CNTs-organic species blend. The success of the latter approach is strongly dependent on appropriate chemical functionalization of CNTs, length-shortening of CNTs, and optimization of their concentration in organic composites. Among the range of chemical functionalization methods available, the acid treatment

* Corresponding author. Tel.: +82 55 350 5287; fax: +82 55 350 5653.
E-mail addresses: sookim@pusan.ac.kr (S.H. Kim), jwkang@kims.re.kr (J.-W. Kang).

0927-0248/$ - see front matter © 2009 Elsevier B.V. All rights reserved.
doi:10.1016/j.solmat.2009.12.018

Author's personal copy

of CNTs results in surface modification from hydrophobic to hydrophilic properties so that they can be blended easily with a solution of photoactive polymers [20]. However, OPV devices employing polymer/CNTs composite thin films as an active layer have not achieved a satisfactory PCE so far. This is because CNTs are poorly dispersed in the polymer matrix, and the length of CNTs ranges from a hundred nm to several μm, which makes them larger than the overall thickness of the photoactive layer so that electrical short circuit occurs.

This paper describes a new method for fabricating OPV with an active layer of a hybrid CNT-doped BHJ polymer-composite thin film, where a homogeneous dispersion of CNTs in a polymer matrix was made and the length of the CNTs was controlled precisely. In this approach, the hybrid CNT–bimetallic composite nanoparticles (hereafter called sea urchin-like CNTs [SU-CNTs]) were made by a combination of conventional spray pyrolysis and thermal chemical vapor deposition (CVD). The SU-CNTs-doped OPV cells without chemical functionalization were also characterized. The resulting SU-CNTs were composed of multi-walled CNTs with a diameter of $\sim 10 \pm 2$ nm and a length of $\sim 200 \pm 40$ nm, which were formed over the entire surface of the bimetallic nanoparticles (Ni/Al) with an average diameter of ~ 150 nm. The OPVs composed of P3HT:PCBM heterojunction solar cells incorporating SU-CNTs showed improved performance compared to the pristine OPV cells.

2. Experimental details

The SU-CNTs were produced by a combination of spray pyrolysis and thermal chemical vapor deposition (CVD) in the gas phase, as described in detail elsewhere [21]. Briefly, aluminum nitrate ($Al(NO_3)_3 \cdot 9H_2O$, Sigma Aldrich) and nickel nitrate ($Ni(NO_3)_3 \cdot 6H_2O$, Sigma Aldrich) were first dissolved in deionized water at a 1:1 molar ratio with a total concentration of ~ 3 wt%. An ultrasonic nebulizer was used to aerosolize the mixed metal nitrate precursor solution. The metal nitrate containing aerosol droplets were then transported rapidly using a controlled amount of nitrogen carrier gas ($< \sim 5$ l pm). After the droplets passed through the subsequent silica-gel dryer, the evaporation-induced metal nitrate solid nanoparticles were formed continuously. The resulting metal nitrate nanoparticles were then mixed with hydrogen gas at a flow rate of ~ 100 sccm in a quartz tube enclosed by an electric furnace and heated to ~ 1000 °C so that the metal nitrate nanoparticles were decomposed thermally into pure bimetallic nanoparticles containing both catalytic nickel (Ni) sites in a noncatalytic aluminum (Al) matrix. These Ni–Al bimetallic nanoparticles formed were then introduced into a quartz reactor enclosed by a second vertically mounted tube furnace, where they were mixed with acetylene (C_2H_2) gas at a flow rate of ~ 15 sccm and heated to ~ 750 °C to grow the CNTs on the surface of the catalytic Ni sites in the bimetallic nanoparticles. In order to obtain short CNTs on the bimetallic particles, the residence time of the seeded bimetallic nanoparticles in the thermal CVD reactor was minimized at ~ 10 s by supplying nitrogen gas with a flow rate of ~ 5 l pm. The resulting hybrid CNT–bimetallic composite particles were finally collected on a membrane filter with a pore size of ~ 200 nm.

The OPV device fabricated on an ITO-coated glass substrate was first cleaned in an ultrasonic bath containing acetone and isopropyl alcohol, and then dried with blowing nitrogen gas. A buffer layer of poly(3,4-ethylenedioxylenethiophene) (PEDOT-PSS, Baytron P):isopropyl alcohol (IPA) (PEDOT-PSS:IPA=1:2) was made using a spin coater after passing through a 0.45 μm filter with a thickness of approximately 40 nm. The coated PEDOT-PSS film was dried at 150 °C for 1 min on a hot plate inside a glove box. The photoactive layer was then deposited by spin-coating a mixture of a SU-CNTs–dispersed P3HT:PCBM(1:1) solution with a thickness of 270 and 560 nm, respectively. A 150-nm-thick aluminum cathode was deposited by thermal evaporation through a shadow mask, which defines a device area of 0.09 cm^2. Finally, the OPV device was thermally annealed at 150 °C for 20 min. The current density–voltage (J–V) characteristics of the OPV devices were measured under AM1.5 simulated illumination with an intensity of 100 mW/cm^2 (Pecell Technologies Inc., PEC-L11 model) [22]. The intensity of sunlight illumination was calibrated using a standard Si photodiode detector with a KG-5 filter. The J–V curves were recorded automatically with a Keithley SMU 2400 source meter by illuminating the OPV cells.

3. Results and discussion

On the basis of the combination of conventional spray pyrolysis and thermal CVD, CNTs were radially grown on the seeded Ni–Al bimetallic particles, which resembled the "sea urchin" structure. The major advantage of hybrid CNT–bimetallic composite particles (i.e., SU-CNTs) is relatively easy to control the length of CNTs with uniform diameter by changing the residence time of bimetallic particles in the thermal CVD reactor. Another advantage is that we can easily make stable suspension of colloidal particles without additional surfactant due to relatively high specific weight of metallic core structure. As shown in Fig. 1, SEM and TEM images confirmed that multi-walled CNTs (i.e., ~ 15 walls) with a diameter of $\sim 10 \pm 2$ nm and a length of $\sim 200 \pm 40$ nm were formed over the entire surface of bimetallic nanoparticles with ~ 150 nm in diameter (see Fig. 1c).

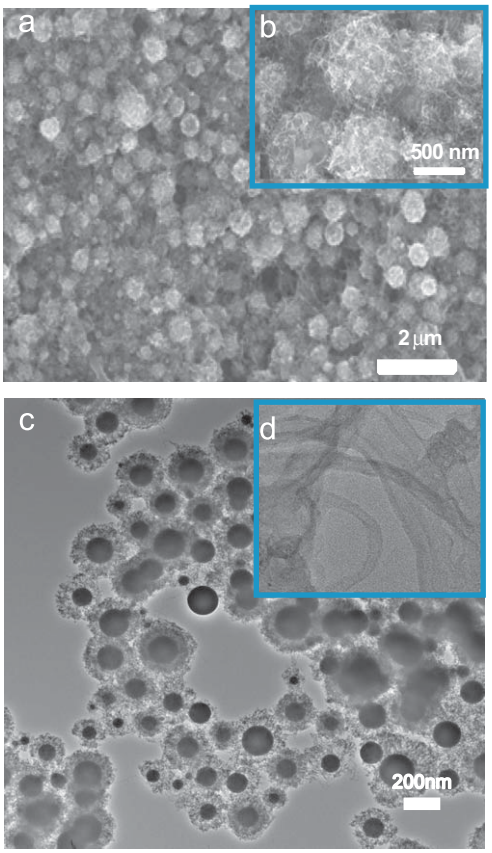

Fig. 1. (a) SEM image of sea urchin-like CNTs ((b) inset: HRSEM image of SU-CNTs) and (c) TEM image of SU-CNTs ((d) inset: HRTEM image of SU-CNTs with ~15 multi-walls).

Author's personal copy

The SU-CNTs formed were then dispersed homogeneously in 1,2-dichlorobenzene without forming severe aggregates by sonication for 1 h with a total mass concentration of ~0.3 mg/mL. 1,2-dichlorobenzene was then added to achieve the desired volume of the diluted CNT solutions. Several series of SU-CNTs-doped P3HT:PCBM (1:1 ratio) solutions were prepared with a relative amount of SU-CNTs to P3HT ranging from 0 to 1.0 wt%. The prepared SU-CNTs-doped P3HT:PCBM solution coated on the surface of ITO-glass by using a spin coater was formed into the active layer. Fig. 2 shows that the SU-CNTs were homogeneously distributed in the polymer matrix without forming severe aggregation.

Fig. 3 shows the absorption spectra of the 230-nm-thick composite thin films with P3HT:PCBM (1:1 ratio) doped with

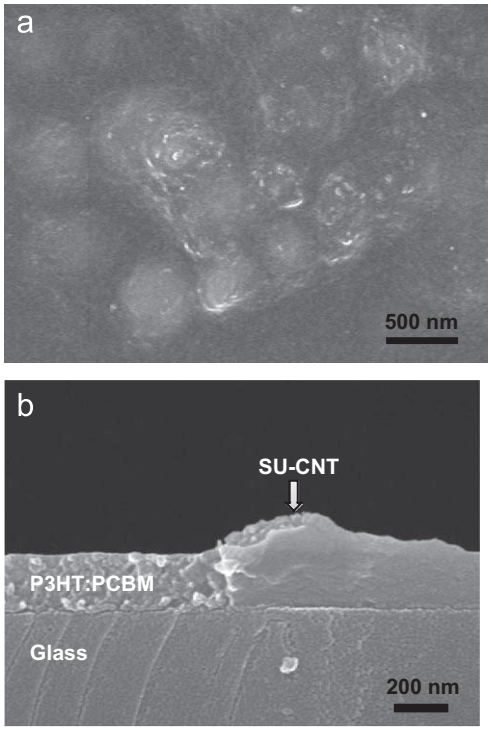

Fig. 2. SEM images of (a) top view and (b) cross-section of a 0.5 wt% SU-CNTs-doped P3HT:PCBM (1:1) film.

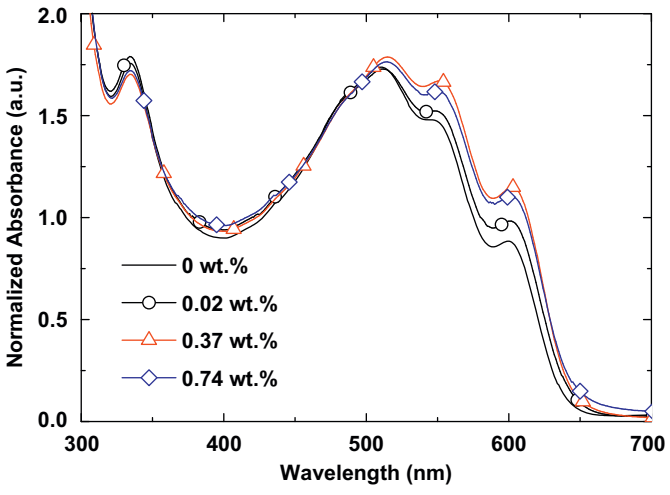

Fig. 3. Normalized absorption spectra of the thin films with the different amount of SU-CNTs doped in the P3HT:PCBM (1:1) composite films.

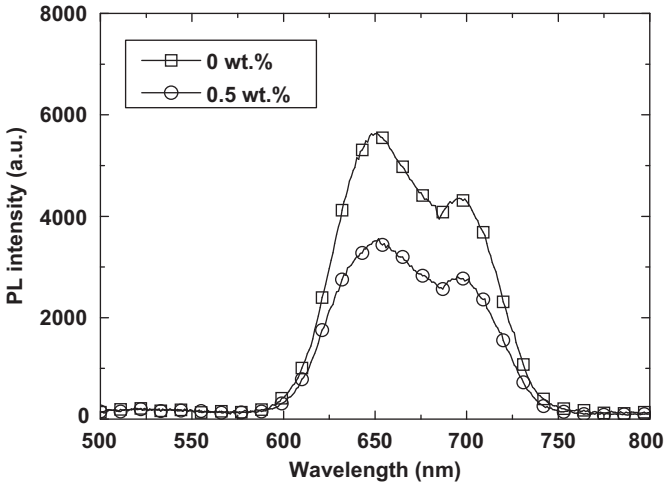

Fig. 4. Photoluminescence (PL) spectra of the P3HT:PCBM thin films with the different doping concentrations of SU-CNTs.

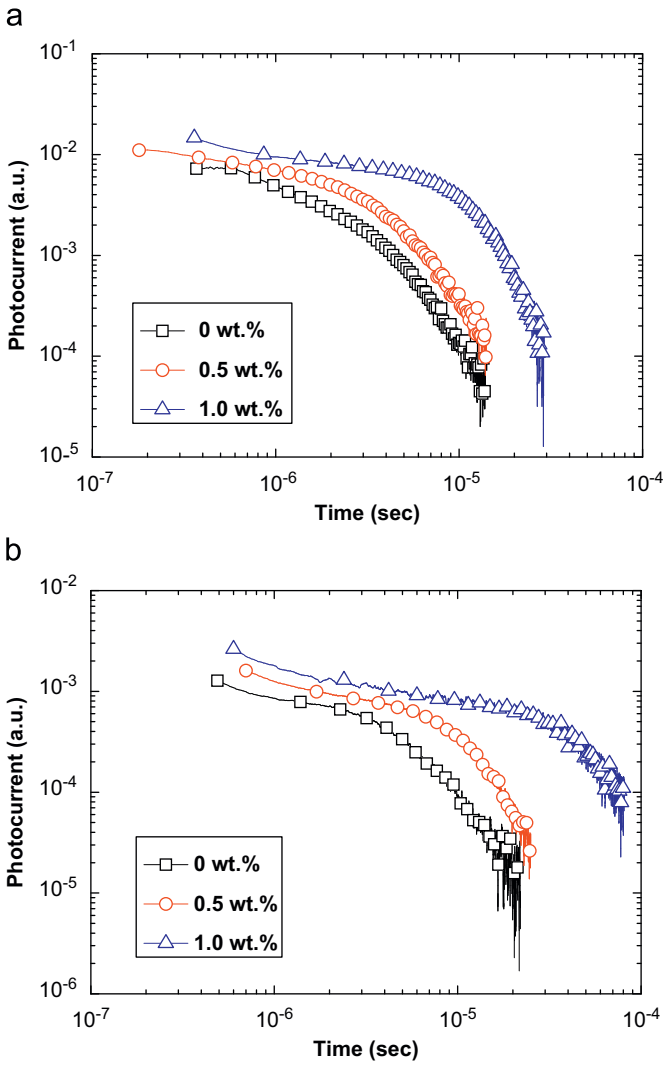

Fig. 5. Double logarithmic plots of (a) electron and (b) hole time-of-flight (TOF) transients in the SU-CNTs-doped P3HT:PCBM films with three different concentrations of SU-CNTs at a applied field of 0.1 MV/cm and room temperature.

Author's personal copy

different amount of SU-CNTs. The absorption spectrum of a mixture of P3HT:PCBM (1:1) mainly shows three peaks: a broad absorption band at 510 nm, and two shoulders at 547 and 598 nm. In the case of the SU-CNTs-doped polymer composite thin films, the originally strong vibronic shoulders show a significant increase in the absorption of red region. Thermally annealed P3HT:PCBM films are reported to have the prominent vibronic features [23], indicating that strong interchain–interlayer reactions among the P3HT chains and polymer ordering are occurring in the blend films. The absorption spectra below the wavelength of 450 nm are very similar for all composite films, indicating that the PCBM absorption is rarely affected by various CNT doping concentrations. Therefore, this suggests that the occurrence of vibronic peaks and strong absorption in the red region is attributed to the structuring between P3HT chains and CNTs [13].

The measurement of photoluminescence (PL) spectra can provide the direct evidence for representing the magnitude of exciton dissociation. Fig. 4 shows PL spectra with and without SU-CNT doping in the P3HT:PCBM film. After doping of 0.5 wt% SU-CNTs, the PL intensity of CNT-doped P3HT:PCBM film was considerably decreased, suggesting that SU-CNTs have strong potentials as exciton dissociating centers.

The effect of SU-CNTs in the P3HT:PCBM film on charge transport properties can be understood by measuring the mobility of electron and hole. From time-of-flight (TOF) measurement [24,25] as shown in Fig. 5, P3HT:PCBM has the averaged electron and hole mobility of $\mu_e = 1.6 \times 10^{-4}$ and $\mu_h = 1.7 \times 10^{-4}\,cm^2\,V^{-1}\,s^{-1}$ at the applied field of 0.1 MV/cm, respectively, which are similar to reported values [25]. As the concentration of SU-CNTs was increased, the electron mobility was accordingly decreased to 1.4×10^{-4} and $1.0 \times 10^{-4}\,cm^2V^{-1}s^{-1}$ for 0.5 and 1.0 wt% SU-CNTs, respectively. However, the hole mobility falls significantly to a value of 1.0×10^{-4} and $0.4 \times 10^{-4}\,cm^2V^{-1}s^{-1}$ for the concentrations of 0.5 and 1.0 wt% SU-CNTs, respectively. The significant reduction in the hole mobility is presumably attributed to the formation of shallow hole traps in the polymer matrix [26]. For P3HT:PCBM films with low concentration of SU-CNTs ($\leq$0.5 wt%), the ratio of electron and hole mobility is close to unity (i.e., μ_e/μ_h=0.94–1.4), which results in balancing the carrier transport in the active layer. When the transport of charges in the 1.0 wt% SU-CNTs-doped P3HT:PCBM layer is unbalanced (i.e., μ_e/μ_h=2.5), the accumulation of hole occurs and the photocurrent is subsequently space-charge limited in the active layer so that it can result in lowering FF values [9].

To evaluate the effect of SU-CNTs on the performance of P3HT:PCBM photoactive layer, the *J–V* characteristics of OPVs were measured under AM 1.5 illumination (100 mW/cm^2) for two different active layer thickness of 270 and 560 nm, respectively, with varying the doping concentration of SU-CNTs as shown in Fig. 6. For two different thicknesses of the active layers, the J_{sc} was increased by increasing the amount of SU-CNTs doping concentration in the photoactive layer. This suggests that the increase of absorption and exciton dissociation resulted from the doping of SU-CNTs is the major factor for enhancing the J_{sc}. In the case of the 270-nm-thick photoactive layer, the V_{oc} and FF were decreased significantly with increasing SU-CNTs concentration (see Fig. 6a). This suggests that short-circuits were made in the OPV devices presumably because the total size of the hybrid Ni–Al bimetallic nanoparticle and CNTs composite exceeded the distance between both electrodes. Therefore, the OPV cell with 0.5 wt% SU-CNTs showed a low PCE of ~1.3%, which is half that obtained from the control device without the SU-CNTs (i.e., PCE~2.61%). In order to eliminate possible short-circuits in the OPV device, we newly introduced thicker photoactive layer up to ~560 nm, which is larger than the total size of SU-CNTs (i.e., < ~550 nm). For the 560-nm-thick photoactive layer with low doping level of SU-CNTs ($\leq$0.5 wt%), the J_{sc} of OPVs was increased from 7.5 to 9.5 mA/cm^2, resulting in

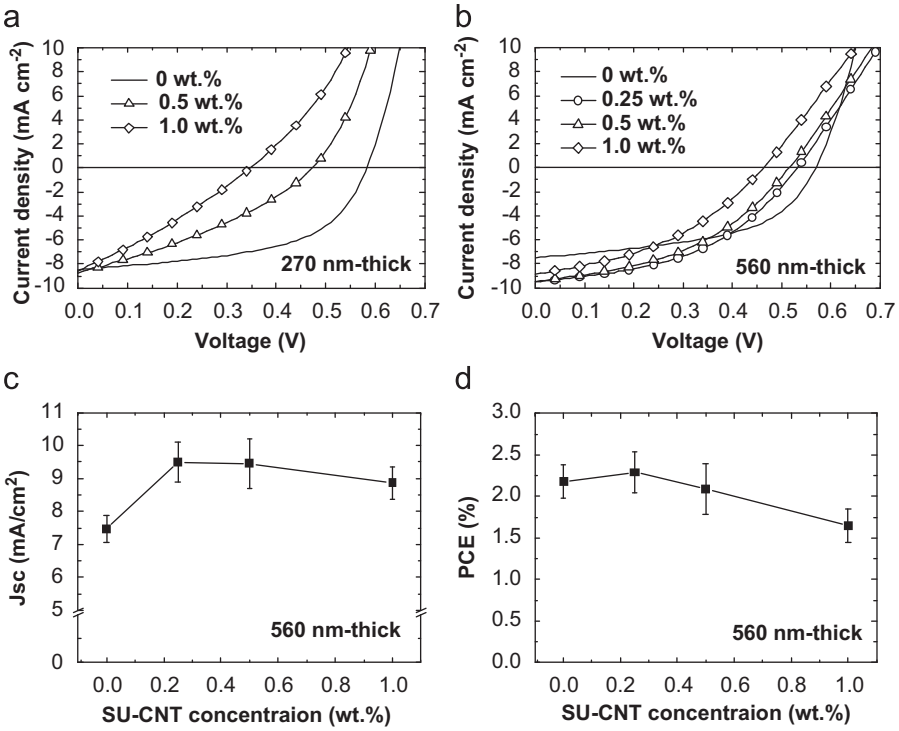

Fig. 6. Current density vs voltage (*J–V*) characteristics of organic photovoltaic cells with (a) 270-nm-thick and (b) 560-nm-thick active layer using various concentrations of SU-CNTs in the P3HT:PCBM (1:1) photoactive layer. (c) Short-circuit current density (J_{sc}) and (d) power conversion efficiency (PCE) as a function of the SU-CNTs concentration in the P3HT:PCBM with 560-nm-thick active layer.

Author's personal copy

slight improvement of the PCE from $2.1 \pm 0.1\%$ to $2.2 \pm 0.2\%$ (max. 2.5%). An increase in the absorption coefficient and exciton dissociation with a balanced ratio of μ_e/μ_h accounts for the enhancement of both the J_{sc} and PCE of the OPV cells. However, in the case of higher SU-CNT doping level (1.0 wt%), the presence of aggregated SU-CNTs in the polymer matrix resulted in decreasing hole mobility due to hole trapping effect, leading to the decrease of the J_{sc} and FF [9,27].

For higher concentration of SU-CNTs (i.e., >0.5 wt%), the photocurrent is limited by the possible combinations of lower photogeneration rates, increased recombination sites, and reduced charge mobilities. In addition, the possible presence of metallic CNTs enhances the recombination of charge carriers. The metallic CNTs with no bandgap play the role of charge trapping and recombination canters in the composite semiconductor medium. Nevertheless, it is noted that the significant increase in J_{sc} with low SU-CNTs doping levels is related to the improved exciton dissociation and absorption coefficient with balanced carrier mobility. This suggests that SU-CNTs employed in this approach are effective exciton dissociation centers in the active layer of polymer/PCBM composites.

4. Conclusions

In this work, we have described a new method to fabricate SU-CNTs doped in bulk heterojuction polymer-fullerene photovoltaic devices. Compared with the pristine OPV device without adding SU-CNTs to the active layer, the SU-CNTs-doped OPV cells showed an improved J_{sc} and PCE. The optimum conditions for achieving the best OPV performance in this approach were obtained with a mixture of P3HT:PCBM (1:1) and 0.25 wt% SU-CNTs, which generated a V_{oc} of 0.532 V, J_{sc} of 9.49 mA/cm^2, FF of 0.454, and a resulting PCE of $\sim$2.2%. This suggests that the specially designed SU-CNTs have a strong potential as an effective exciton dissociation medium in the polymer active layer to enhance the performance of organic photovoltaic cells.

Acknowledgement

This work was supported by the Korea Foundation for International Cooperation of Science and Technology (KICOS) through a grant provided by the Korean Ministry of Education, Science & Technology (MEST) in K20701010289-07B0100-07500.

References

[1] C.W. Tang, Two-layer organic photovoltaic cell, Appl. Phys. Lett. 48 (1986) 183–185.
[2] F.C. Krebs, M. Jørgensen, K. Norrman, O. Hagemann, J. Alstrup, T.D. Nielsen, J. Fyenbo, K. Larsen, J. Kristensen, A complete process for production of flexible large area polymer solar cells entirely using screen printing—first public demonstration, Sol. Energy Mater. Sol. Cells 93 (2009) 422–441.
[3] F.C. Krebs, Polymer solar cell modules prepared using roll-to-roll methods: knife-over-edge coating, slot-die coating and screen printing, Sol. Energy Mater. Sol. Cells 93 (2009) 465–475.
[4] M. Jørgensen, K. Norrman, F.C. Krebs, Stability/degradation of polymer solar cells, Sol. Energy Mater. Sol. Cells 92 (2009) 686–714.
[5] F.C. Krebs, S.A. Gevorgyan, J. Alstrup, A roll-to-roll process to flexible polymer solar cells: model studies, manufacture and operational stability studies, J. Mater. Chem. 19 (2009) 5442–5451.
[6] R. Kroon, M. Lenes, J.C. Hummelen, P.W.M. Blom, B. de Boer, Small bandgap polymers for organic solar cells (polymer material development in the last 5 years), Polym. Rev. 48 (2008) 531–582.
[7] B.C. Thompson, J.M.J. Fréchet, Polymer-fullerene composite solar cells, Angew. Chem. Intl. Ed 47 (2008) 58–77.
[8] W.L. Ma, C.Y. Yang, X. Gong, K. Lee, A.J. Heeger, Thermally stable efficient polymer solar cells with nanoscale control of the interpenetrating network morphology, Adv. Funct. Mater. 15 (2005) 1617–1622.
[9] G. Li, V. Shrotriya, J.S. Huang, Y. Yao, T. Moriaty, K. Emery, Y. Yang, High-efficiency solution processable polymer photovoltaic cells by self-organization of polymer blends, Nat. Mater. 4 (2005) 864–868.
[10] S.H. Park, A. Roy, S. Beaupré, S. Cho, N. Coates, J. Sun Moon, D. Moses, M. Leclerc, K. Lee, A.J. Heeger, Bulk heterojunction solar cells with internal quantum efficiency approaching 100%, Nat. Photonics 3 (2009) 297–302.
[11] J.Y. Kim, K. Lee, N.E. Coates, D. Moses, T.Q. Nguyen, M. Dante, A.J. Heeger, Efficient tandem polymer solar cells fabricated by all-solution processing, Science 317 (2007) 222–225.
[12] M.C. Scharber, D. Wuhlbacher, M. Koppe, P. Denk, C. Waldauf, A.J. Heeger, C.L. Brabec, Design rules for donors in bulk-heterojunction solar cells-towards 10% energy-conversion efficiency, Adv. Mater. 18 (2006) 789–794.
[13] S. Berson, R. Bettignies, S. Bailly, S. Guillerez, B. Jousselme, Elaboration of P3HT/CNT/PCBM composites for organic photovoltaic cells, Adv. Funct. Mater. 17 (2007) 3363–3370.
[14] M.W. Rowell, M.A. Topinka, M.D. McGehee, H.J. Prall, G. Dennler, N.S. Sariciftici, L. Hu, G. Gruner, Organic solar cells with carbon nanotube network electrodes, Appl. Phys. Lett. 88 (2006) 233506-1-233506-3.
[15] J.V. Lagemaat, T.M. Barnes, G. Rumbles, S.E. Shaheen, T.J. Coutts, C. Weeks, I. Levitsky, J. Peltola, P. Glatkowski, Organic solar cells with carbon nanotubes replacing In2O3:Sn as the transparent electrode, Appl. Phys. Lett. 88 (2006) 233503-1-233503-3.
[16] A.D. Pasquier, H.E. Unalan, A. Kanwal, S. Miller, M. Chhowalla, Conducting and transparent single-wall carbon nanotube electrodes for polymer-fullerene solar cells, Appl. Phys. Lett. 87 (2005) 203511-1-203511-3.
[17] S. Chaudhary, H. Lu, A.M. Muller, C.J. Bardeen, M. Ozkan, Hierarchical placement and associated optoelectronic impact of carbon nanotubes in polymer-fullerene solar cells, Nano Lett. 7 (2007) 1973–1979.
[18] B. Pradhan, S.K. Batabyal, A.J. Pal, Functionalized carbon nanotubes in donor/acceptor-type photovoltaic devices, Appl. Phys. Lett. 88 (2006) 093106-1-093106-3.
[19] P.R. Somani, S.P. Somani, M. Umeno, Application of metal nanoparticles decorated carbon nanotubes in photovoltaics, Appl. Phys. Lett. 93 (2008) 033315-1-033315-3.
[20] A.J. Miller, R.A. Hatton, S.R.P. Silva, Interpenetrating multiwall carbon nanotube electrodes for organic solar cells, Appl. Phys. Lett. 89 (2006) 133117-1-133117-3.
[21] Y.K. Moon, J.B. Lee, J.K. Lee, T.G. Kim, S.H. Kim, Synthesis of length-controlled aerosol carbon nanotubes and their dispersion stability in aqueous solution, Langmuir 25 (2009) 1739–1743.
[22] J.W. Kang, S.P. Lee, D.G. Kim, S. Lee, J.K. Kim, S.Y. Park, J.H. Kim, H.K. Kim, Reduction of series resistance in organic photovoltaic using low sheet resistance of ITO electrode, Electrochem. Solid-State Lett. 12 (2009) H64–H66.
[23] A. Ikeda, K. Nobusawa, T. Hamano, J. Kikuchi, Single-wall carbon nanotubes template the one-dimensional ordering of a polythiophene derivative, Org. Lett. 8 (2006) 5489–5492.
[24] J. Huang, G. Li, Y. Yang, Influence of composition and heat-treatment on the charge transport properties of poly(3-hexylthiophene) and [6,6]-phenyl C61-butyric acid methyl ester blends, Appl. Phys. Lett. 87 (2005) 112105-1-112105-3.
[25] J.-W. Kang, S.-H. Lee, H.-D. Park, W.-I. Jeong, K.-M. Yoo, Y.-S. Park, J.-J. Kim, Low roll-off of efficiency at high current density in phosphorescent organic light emitting diodes, Appl. Phys. Lett. 90 (2007) 223508-1-223508-3.
[26] J.-H. Xu, J. Shen, Effects of discrete trap levels on carrier transport in organic electroluminescent devices, J. Appl. Phys 83 (1998) 2646–2648.
[27] E. Kymakis, P. Servati, P. Tzanetakis, E. Koudoumas, N. Kornilios, I. Rompogiannakis, Y. Franghiadakis, G.A.J. Amaratunga, Effective mobility and photocurrent in carbon nanotube-polymer composite photovoltaic cells, Nanotechnology 18 (2007) 435702-1-435702-6.